Noeloikeau Charlot

ncharlot@hawaii.edu

9/27/2016

University of Hawaii

PHYS480L

Gamma Ray Angular Dependence of ^{22}Na and ^{60}Co Emissions

Abstract:

The objective of this experiment is to predict and measure the angular dependencies of photons resulting from decays in ^{22}Na and ^{60}Co sources. Time coincidence techniques were employed using fast electronics to measure coincident photons for both elements, confirming theoretical expectations regarding the angular distribution of each primary decay chain.

Backround:

Radioactive materials emit particles as they decay to lower, more stable energy states. These emissions can be detected using fast electronics, possessing applications ranging from particle physics to medical imaging. One such example is Positron Emission Tomography, or PET, a routine procedure used to image tissue dynamically. This technology relies on a concept known as *β^+-decay*.

When a radionuclide decays to a lower energy state, it may do so with a high probability of releasing one or more charged particles. In γ decay, a radionuclide emits a gamma ray as it transitions to a more stable configuration. In *β-decay*, either an electron or its antiparticle (positron) is emitted.

In the presence of a surrounding medium such as the atmosphere, a β^+ positron annihilates with an ambient electron according to $e^+ + e^- \rightarrow \gamma + \gamma$. Described pictorially,

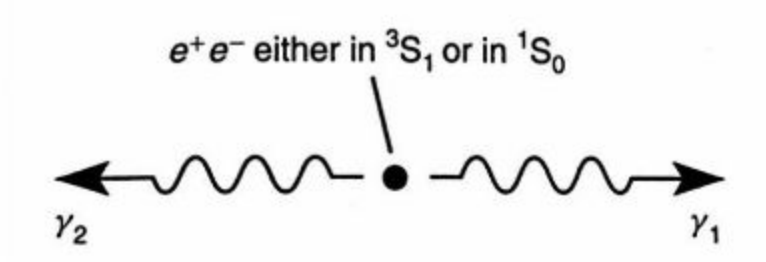

Figure 1: Two photon emission as a result of electron-positron annihilation. [1]

By conservation of momentum the gamma rays are emitted in antiparallel directions along the line of collision. This condition is equivalent to stating their relative angular distribution function $C(\theta) = \delta(\theta - \pi).$ The β decay process was observed in the Na^{22} decay chain below to the left, while an anisotropic γ decay was observed for Co^{60}, to the right

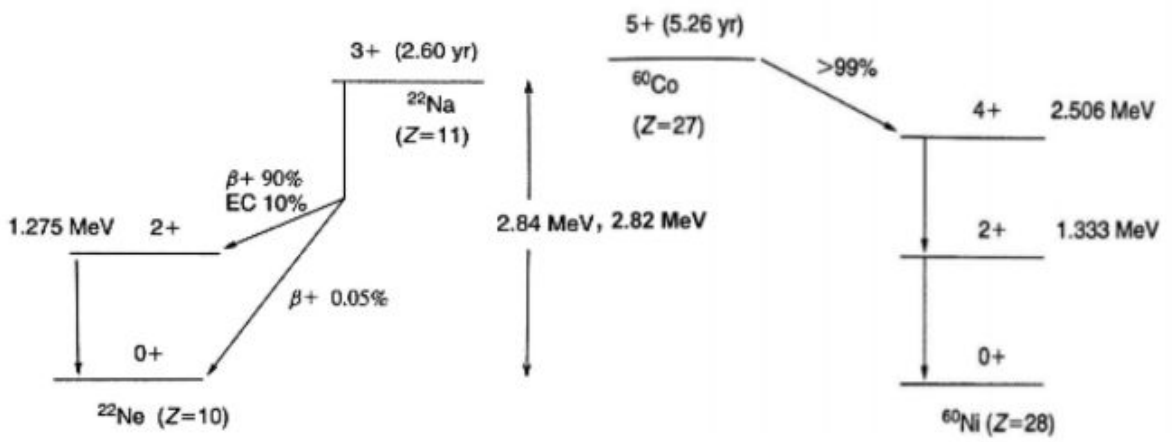

Figure 2: Decay schemes of ^{22}Na (left) and ^{60}Co (right). [1]

The ^{22}Na decay chain with the highest probability (>90%) is described by the pathway $^{22}Na \rightarrow {}^{22}Ne^{*} + e^{+} + \nu_e$. It is assumed the line of each emission is uniformly distributed across all possible solid angles.

Apparatus:

Equidistant, antiparallel detectors were used to observe the annihilation events described above. The experimental apparatus consisted of two NaI(Tl) scintillation crystal detectors attached to photomultiplier tubes and a logic circuit, itself composed of discriminators, a delay box, coincidence unit, and scaler (counter), the block diagram of which is given below:

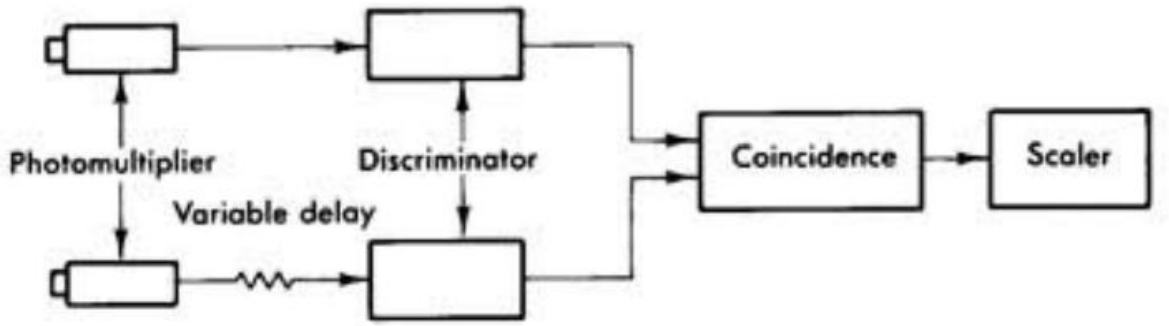

Figure 3: Block diagram of experimental circuit. Arrows indicate direction of signal propagation. *[1]*

The essential mechanism of the circuit begins when a single photon interacts with the face of an individual detector. A signal then passes through the photomultiplier tube behind the detector face, and after some delay the discriminator reads the signal from the photomultiplier. If the signal has reached the specified voltage threshold then it is passed from the discriminator. When the signals from both discriminators are passed to the coincidence unit within the specified time interval, the scaler increments the coincidence count, and the process is repeated.

Procedure:

The source was placed an equal distance between the two detectors with one detector held stationary as the other was rotated incrementally, sweeping through an angle of 90° and pictured at a single point in time below.

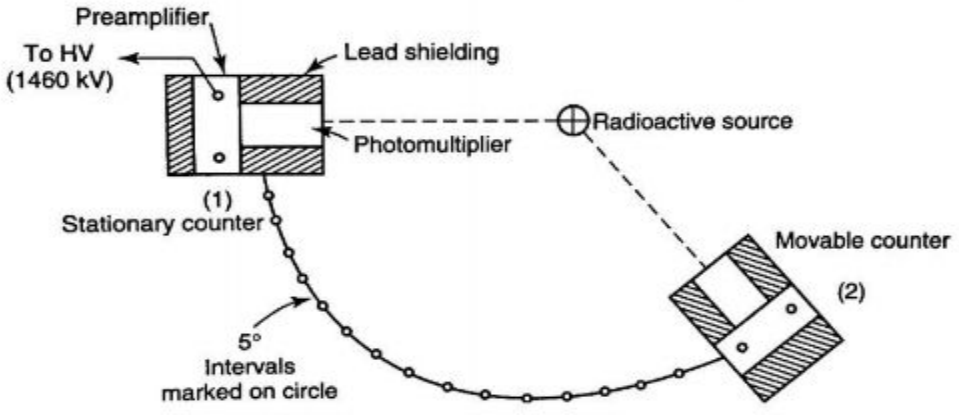

Figure 4: Rochester experimental apparatus undergoing rotation. [1] Actual device used did not include lead shielding, and used 3 degree increments.

The distance from each detector to the source was held constant throughout each measurement set. A total of three distinct angular distribution measurements of ^{22}Na and one angular distribution measurement of ^{60}Co were taken in this way.

Calculations:

The rate of accidental coincidences in the circuit $R_{accidental} = R_1 R_2 \Delta t$, where R_i is the rate of accidentals from detector i and Δt is the discriminator output pulse width.

The observed ^{22}Na angular distribution was fit to a Gaussian with a constant offset of the form $f_1(\theta) = \frac{d}{\sigma\sqrt{2\pi}} exp[-(\theta - \theta_0)/(2\sigma^2)] + c,$ having standard deviation $\sigma = (2\sqrt{2ln2})^{-1} FWHM$.

The observed ^{60}Co angular distribution was fit to a cosine with an integer offset of the form: $f_2(\theta) = 1 + a \cdot cos^2(\theta)$, in which the constant a was fit explicitly.

The equation used to describe the overlapping area of the detector faces is of the form: $f_3(\varphi) = 2R^2[cos^{-1}(|\varphi|) - |\varphi|\sqrt{1-\varphi^2}]$, where $\varphi = \frac{L \cdot sin(\theta)}{4R}$ is introduced for convenience and where L, R, θ are the initial distance between antiparallel detector faces, the radius of each detector face, and the angular separation of the detectors, respectively. The resolving time of the circuit

was estimated from the width of a delay curve representing the coincidence counts from the ^{22}Na source. The actual resolving time of the circuit was determined from the full-width at half maximum of f_3 for each distance configuration by using the FindRoot function in Mathematica. The error associated with counts themselves was estimated according to a Poisson distribution in which the magnitude of the standard deviation is given by the square root of the number of measurements, i.e, $\delta f = \sqrt{N}$ where δf is the error of the function f having N measurements.

Data:

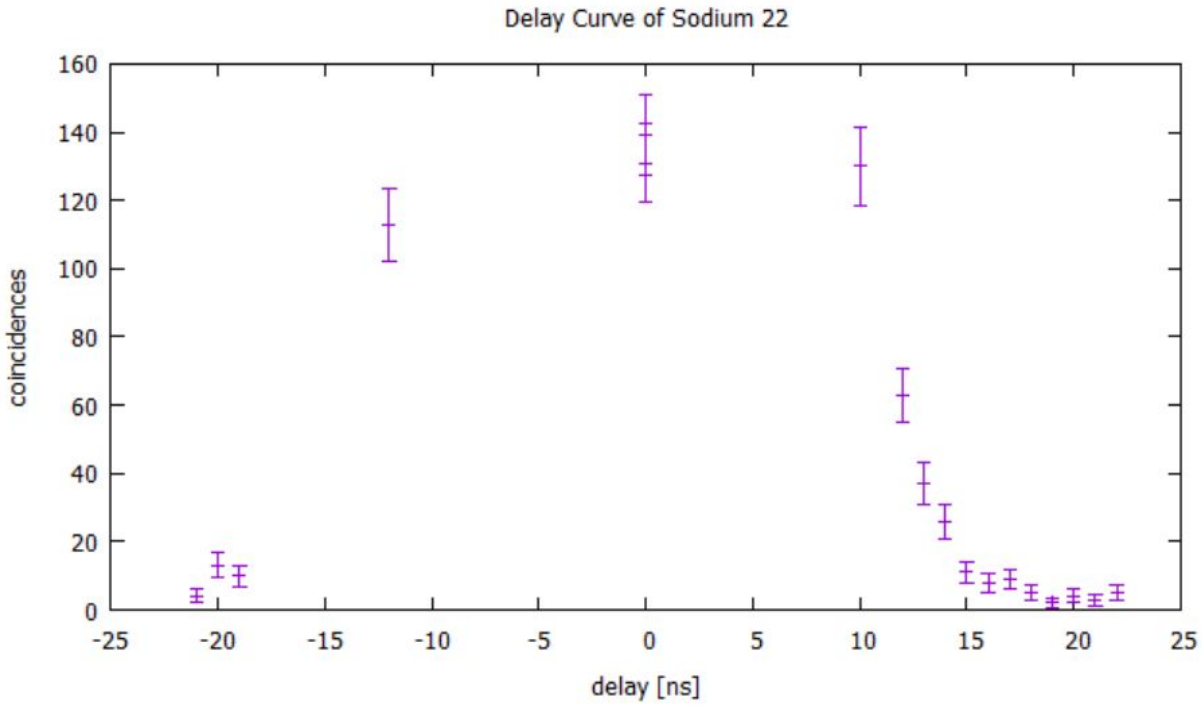

Figure 5: ^{22}Na delay curve representing temporal separation permitted by coincidence unit.

$R_{accidental} = 0.00018 s^{-1} = 0.643 hr^{-1}$

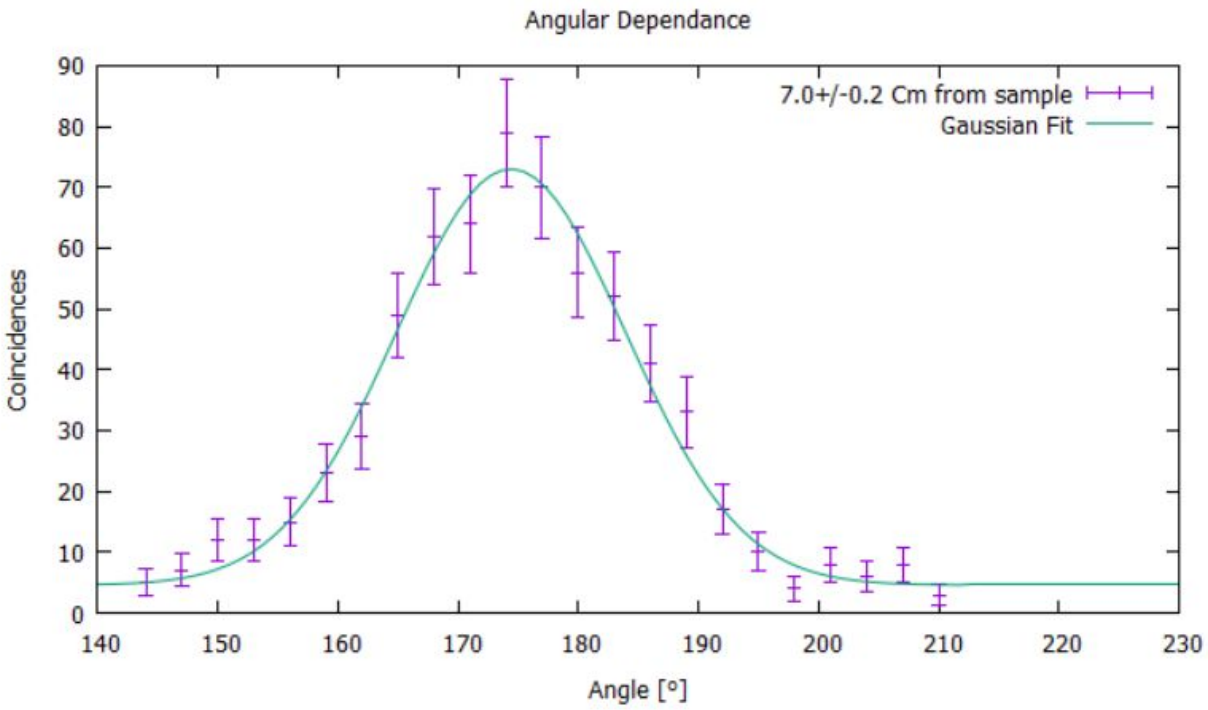

Figure 6: Angular distribution of ^{22}Na emissions with $L = 14 \pm 0.4cm$.

$FWHM_{Gaussian\ Fit} = 22.26°$

$FWHM_{Theoretical} = 27.33°$

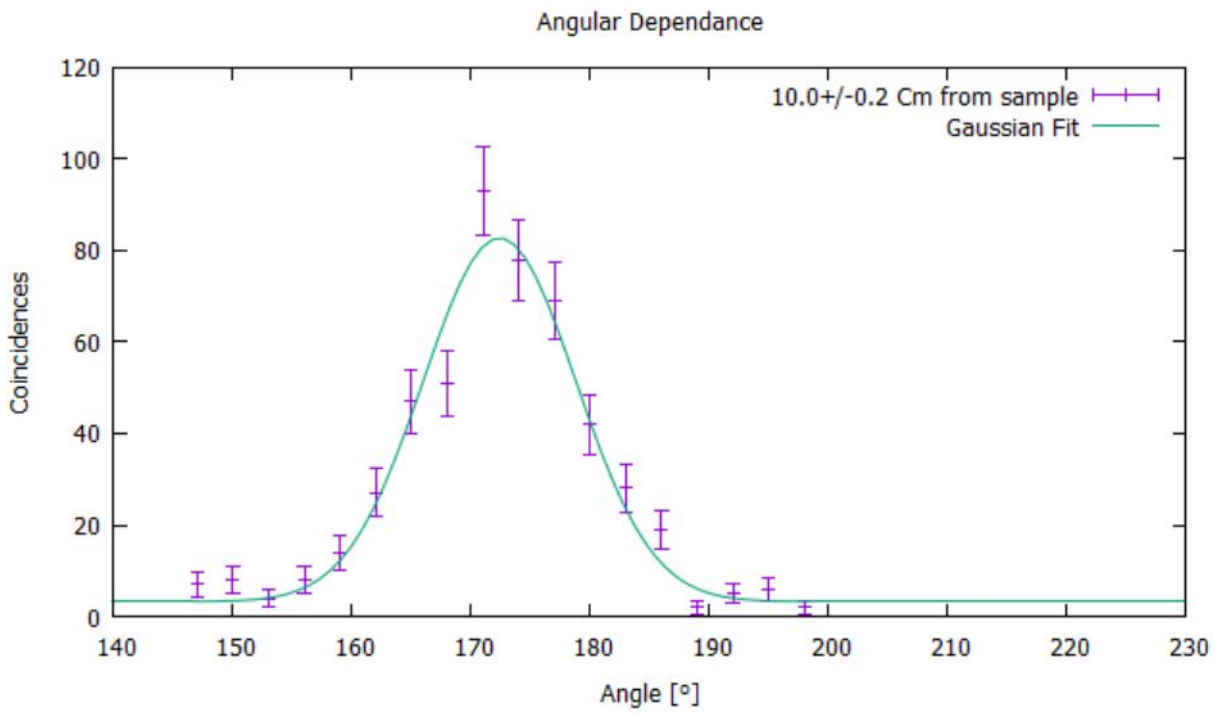

Figure 7: Angular distribution of ^{22}Na emissions with $L = 20 \pm 0.4cm$.

$FWHM_{Gaussian\ Fit} = 14.47°$

$FWHM_{Theoretical} = 19.08°$

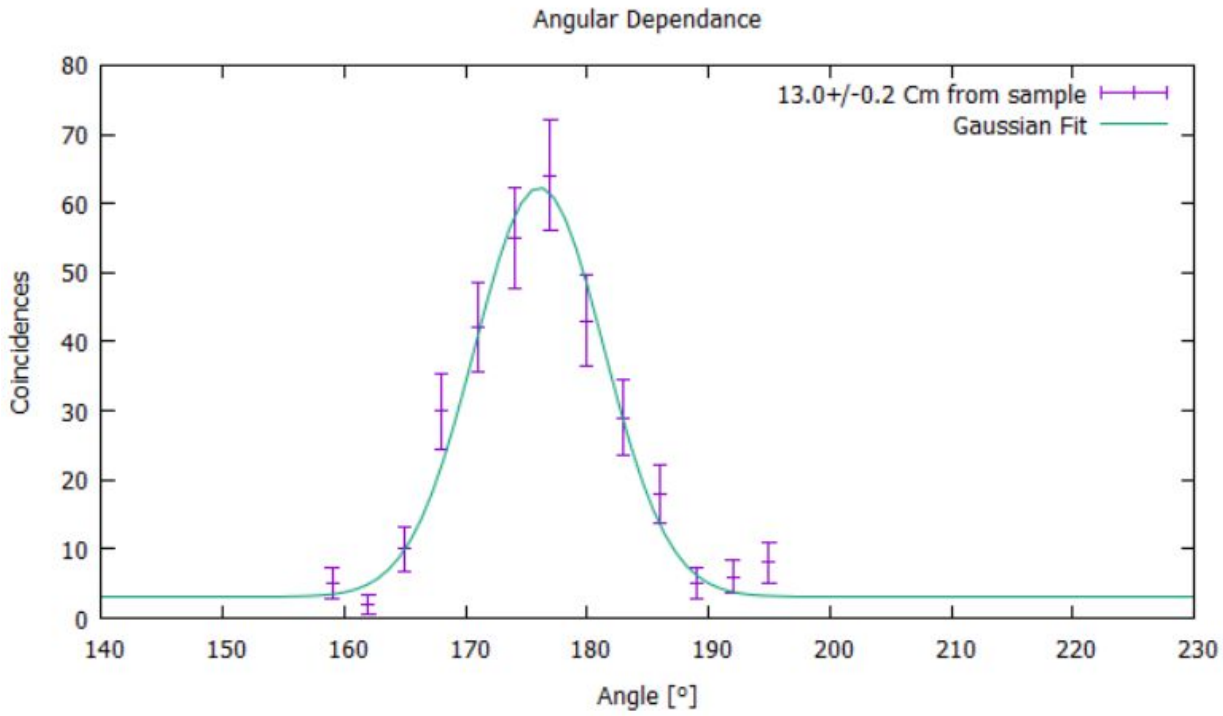

Figure 8: Angular distribution of ^{22}Na emissions with $L = 26 \pm 0.4cm$.

$FWHM_{Gaussian\ Fit} = 12.88°$

$FWHM_{Theoretical} = 14.67°$

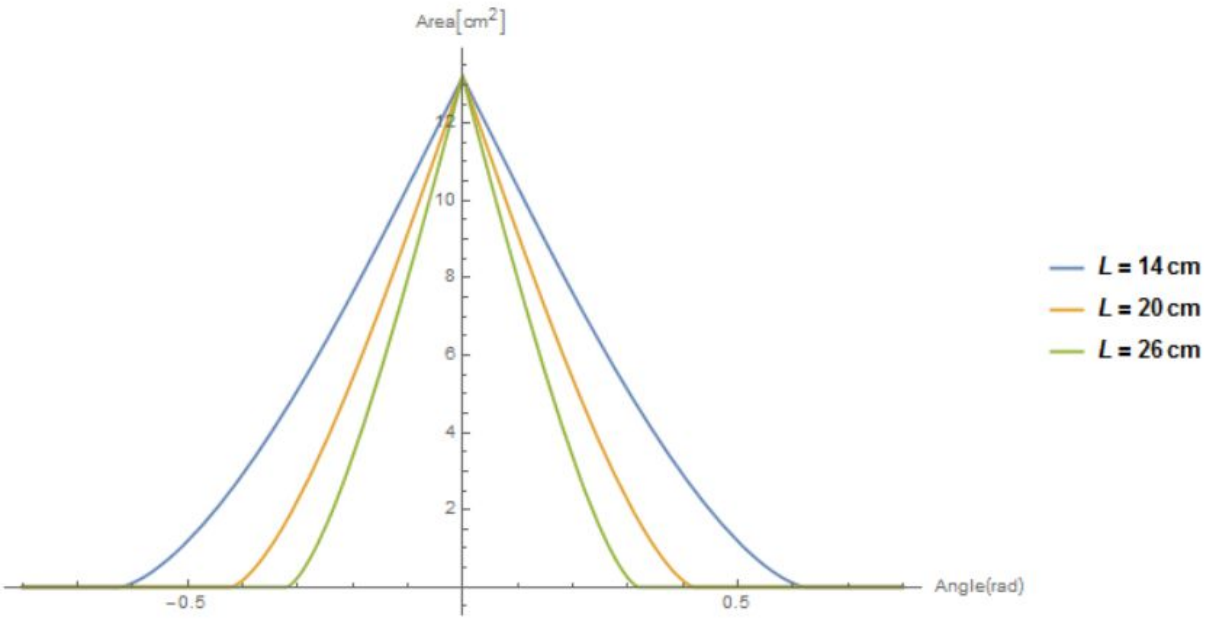

Figure 9: Overlap of detector faces as a function of linear and angular separation for all three ^{22}Na trails. Each curve represents a different linear separation corresponding to the three cases above.

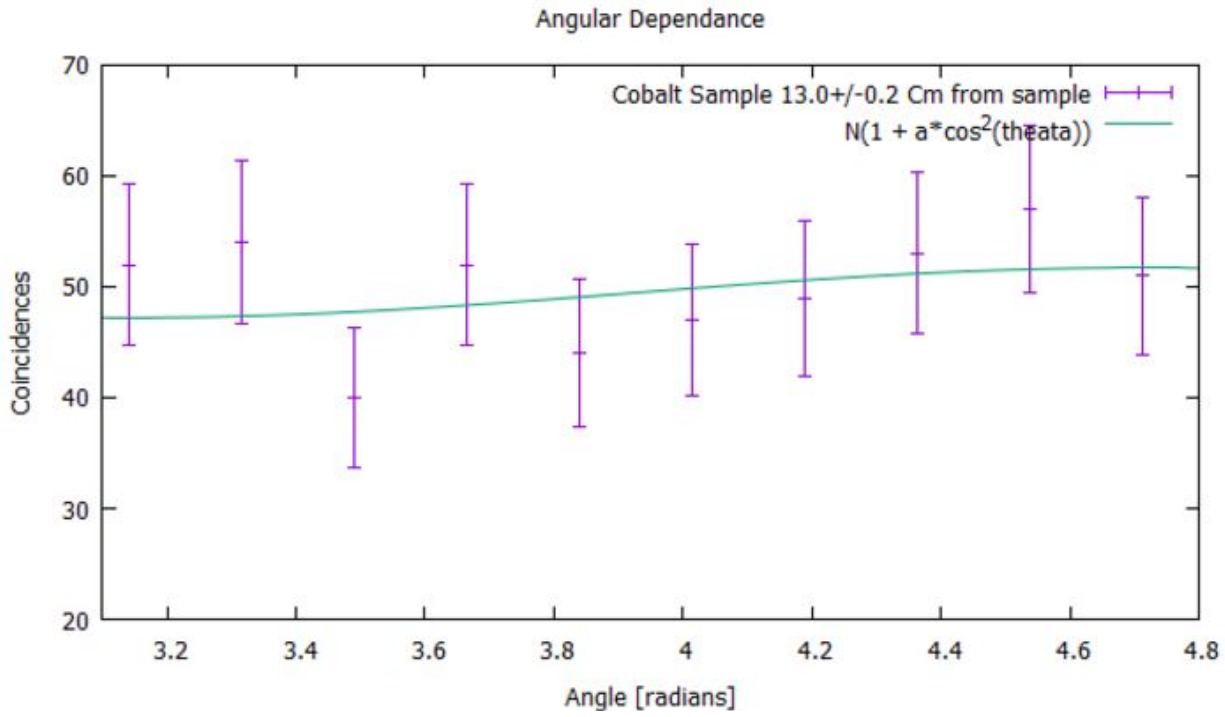

Figure 10: Angular distribution of ^{60}Co emissions with $L = 26 \pm 0.4cm$.

Discussion:

The calculated accidentals rate is negligible in relation to the number of counts considered. The observed angular distributions were displaced in each case from the expected peak at 190°, which can be understood a result of the detector itself being misaligned in each case. The FWHM values calculated from the Gaussian fit were in all cases several degrees smaller than the theoretical prediction. This can be understood as a consequence of the curve bounding the theoretical prediction being inherently wider than the Gaussian used to fit the experimental data.

The ^{60}Co distribution fit displays an anisotropic angular dependence, with the amplitude of oscillation centered about ~50 counts and varying by approximately ~2 counts above and below this value. This matches the anisotropic behavior expected from theoretical considerations.

Conclusion:

Angular dependencies of gamma ray emissions resulting from ^{22}Na and ^{60}Co electron-positron annihilation were measured using fast electronics. The resulting distributions were fit to theoretical approximations and found to be in strong agreement in both the ^{22}Na and ^{60}Co data.

References:

[1]: Melissinos, A. Experiments in Modern Physics, First Edition. New York Academic Press. Chapter 9. Accessed 9/26/2016.

Collaborators:

[1]: John Adamski,

[2]: Carly Hall,

[3]: Hendrik Mol.